ORGANOMETALLICS

Article

pubs.acs.org/Organometallics

Hydrolysis and Methanolysis of Silanes Catalyzed by Iridium(III) Bis-N-Heterocyclic Carbene Complexes: Influence of the Wingtip Groups

Mélanie Aliaga-Lavrijsen,[†] Manuel Iglesias,*[,†] Andrea Cebollada,[†] Karin Garcés,[†] Nestor García,[‡] Pablo J. Sanz Miguel,[†] Francisco J. Fernández-Alvarez,*[,†] Jesús J. Pérez-Torrente,[†] and Luis A. Oro*[,†,‡]

[†]Departamento de Química Inorgánica-Instituto de Síntesis Química y Catálisis Homogénea (ISQCH), Universidad de Zaragoza-CSIC, 50009 Zaragoza, Spain

[‡]Center for Refining and Petrochemicals and Department of Chemistry, King Fahd University of Petroleum and Minerals, Dhahran 31261, Saudi Arabia

Supporting Information

ABSTRACT: New $[Ir(CH_3CN)_2(I)\{\kappa C,C'\text{-bis(NHC)}\}]BF_4$ complexes featuring bis-NHC ligands with a methylene bridge and different N substitution ($-CH_2CH_2CH_2CH_3$ and $-CH_2CH_2OPh$) were synthesized. NMR studies and X-ray diffraction structures evidenced that the wingtip group $-CH_2CH_2OPh$ presents a hemilabile behavior in solution, with the oxygen atom coordinating and dissociating at room temperature, which contrasts with the strong coordination of the ether functions in the complex $[Ir(I)_2\{\kappa C,C',O,O'\text{-bis(NHC}^{OMe})\}]BF_4$ (bis(NHC^{OMe}) = methylenebis(*N*,*N*′-bis(2-methoxyethyl)imidazol-2-ylidene)), previously reported by us. These complexes proved to be efficient catalysts for the hydrolysis and methanolysis of silanes, affording molecular hydrogen and silyl alcohols or silyl ethers as the main reaction products in excellent yields. The hydrogen generation rates were very much dependent on the nature of the hydrosilane and the coordination ability of the wingtip group. The latter also played a key role in the recyclability of the catalytic system.

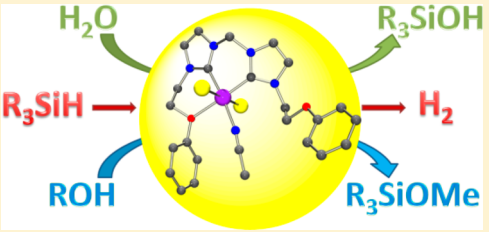

INTRODUCTION

The metal-catalyzed hydrolysis of hydrosilanes is an atom-economical route to silanols, which can be prepared selectively under mild conditions as the only reaction products together with molecular hydrogen. The synthetic relevance of silanols as building blocks for a variety of organic transformations, including cross-coupling reactions and production of silicon-based polymeric materials,[1] illustrates the importance of this reaction. Although the production of silanols and silyl ethers by hydrolysis or of the latter by alcoholysis of Si−H bonds have been extensively studied,[2] the use of organosilanes as potential hydrogen storage agents has been relatively unexplored.[3] A variety of hydrogen storage candidates have been proposed in the literature for the implementation of a hydrogen-based economy.[4] In the last few decades many efforts have focused on the development of fuel cells based on chemical hydrides, ammonia−borane and borohydrides being particularly promising due to their stability and efficient hydrogen production under mild conditions.[5] However, the use of solvents is required in both cases, as they are solids at room temperature, which significantly lowers their hydrogen weight percent and hampers their potential use in fuel cells. Organosilanes, on the other hand, are usually liquids at room temperature, and their boiling point and hydrogen weight percent can be easily tuned by modifying their structure: e.g., 1,3,5-trisilacyclohexane is a cyclic organosilane, liquid at room temperature, that contains three SiH_2 units and has a boiling point of 142 °C.[3d] The hydrolysis or alcoholysis of Si−H bonds is a thermodynamically favorable but kinetically slow process; therefore, the use of a catalyst is essential for an efficient release of molecular hydrogen from organosilanes. Iridium complexes have shown good activities in both the hydrolysis and alcoholysis of a range of hydrosilanes under mild conditions.[2d,3a] In this work we have focused on the development of iridium(III) complexes stabilized with chelating bis-N-heterocyclic carbene (NHC) ligands aiming at the preparation of active and robust catalysts for the production of hydrogen from hydrosilanes. The use of NHCs as spectator ligands in homogeneous catalysis has met with great success in the past two decades. The remarkable performance of NHCs as ancillary ligands has generally been attributed to the stability provided by the covalent character of the $M-C_{carbene}$ bond and to their electronic and steric capabilities.[6] NHCs are strong σ-donor ligands that render highly electron rich metal centers.[7] Moreover, the straightforward modification of the N substituents permits the preparation of NHCs featuring functionalized wingtip groups. Thus, fine tuning of the activity and stability of the catalyst can be achieved by the introduction of wingtip groups with different coordination abilities.

Here we report on the catalytic activity of $[Ir(CH_3CN)_2(I)_2\{\kappa C,C'\text{-bis(NHC)}\}]BF_4$ complexes in the meth-

Special Issue: Mike Lappert Memorial Issue

Received: November 20, 2014

DOI: 10.1021/om5011726
Organometallics XXXX, XXX, XXX−XXX

anolysis and hydrolysis of organosilanes. The methylene-bridged bis-NHC ligands feature N substituents with different coordination abilities ($-CH_2CH_2CH_2CH_3$, $-CH_2CH_2OPh$, and $-CH_2CH_2OMe$). The coordination behavior of the ligands and the relationship between structure and catalytic activity of the complexes was investigated.

RESULTS AND DISCUSSION

Synthesis and Characterization of Bis-Imidazolium Salts. Bis-imidazolium salts **1a,c** were synthesized according to a known literature procedure.[8−10] Methylenebis(*N*,*N*′-bis(2-phenoxyethyl)imidazolium) iodide (**1b**) was prepared likewise by the reaction of 1-(2-phenoxyethyl)-1*H*-imidazole with 0.5 equiv of diiodomethane in refluxing acetonitrile and isolated as a white solid (Scheme 1) upon precipitation from the reaction mixture using diethyl ether.

Scheme 1. Preparation of Bis-Imidazolium Salts 1a−c and Complexes 2a−c

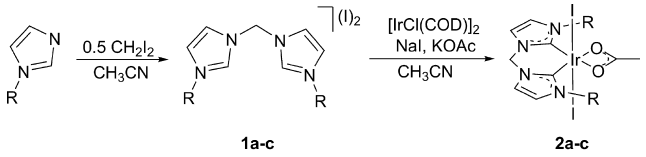

1a-c 2a-c

R = -$CH_2CH_2CH_2CH_3$ (**a**), -CH_2CH_2OPh (**b**), -$CH_2CH_2OCH_3$ (**c**),

^{1}H NMR spectra of **1b** in acetonitrile-d_3 show a resonance corresponding to the NC*H*N protons at δ 9.69 ppm. The protons corresponding to the imidazole rings (NC*H*s) appear as multiplets centered at δ 7.94 and 7.58 ppm. The resonance assigned to the protons of the methylene bridge is observed as a singlet at δ 6.81 ppm. The $-NCH_2-$ and $-OCH_2-$ resonances appear as multiplets centered at δ 4.60 and 4.32 ppm, respectively. In the $^{13}C\{^1H\}$ NMR spectra the most significant signals are those corresponding to the N*C*HN and methylene bridge carbons, which appear as singlets at δ 138.8 and 58.5 ppm, respectively.

Synthesis and Characterization of Complexes 2a−c. The synthesis of complexes **2a,c** have been previously described in the literature.[8−10] In a modified procedure, complex [Ir(κ^2*O*,*O*′-CH_3COO)(I)$_2$\{κ^2*C*,*C*′-bis(NHC)\}] (**2b**; bis-NHC = methylenebis(*N*,*N*′-bis(2-phenoxyethyl)imidazol-2-ylidene)) was prepared by refluxing **1b** with 0.5 equiv of [Ir(μ-Cl)(cod)]$_2$ (cod = 1,5-cyclooctadiene) and an excess of sodium iodide and potassium acetate. The reaction mixture was refluxed for 3 days and monitored by the disappearance of the NC*H*N peak of the bis-imidazolium salt in the ^{1}H NMR. After this period the solvent was evaporated and the residue extracted in dichloromethane. The insoluble inorganic salts were filtered off, and the complex was isolated as an air-stable orange solid in 87% yield after evaporation of the solvent.

The ^{1}H NMR spectra of complex **2b** in CD_2Cl_2 show a singlet corresponding to the methylene bridge at δ 6.11 ppm. The protons assigned to the $-CH_2N-$ and $-CH_2O-$ resonances appear as multiplets centered at δ 4.83 and 4.40 ppm, respectively. The coordination of the acetato ligand was confirmed by the presence of a singlet at δ 2.01 ppm that belongs to the methyl group. In the $^{13}C\{^1H\}$ NMR spectra the most prominent resonances are those corresponding to the two carbene carbons, which appear as a singlet at δ 158.9 ppm, and the η^2-coordinated acetato ligand that shows two peaks at δ 26.6 and 189.8 ppm for the CH_3 and *C*OO carbons, respectively.

Synthesis and Characterization of Complexes 3a,b. Bis-acetonitrile adducts [Ir(CH_3CN)$_2$(I)$_2$\{κ^2*C*,*C*′-bis(NHC^{Bu})\}]BF_4 (**3a**; NHC^{Bu} = methylenebis(*N*,*N*′-di-*n*-butylimidazol-2-ylidene)) and [Ir(CH_3CN)$_2$(I)$_2$\{κ^2*C*,*C*′-bis(NHC^{OPh})\}]BF_4 (**3b**; NHC^{OPh} = methylenebis(*N*,*N*′-bis(2-phenoxyethyl)imidazol-2-ylidene)) were prepared by reaction of **2a,b** with 1.1 equiv of HBF_4·Et_2O in CH_2Cl_2 at 0 °C, followed by addition of excess acetonitrile to the reaction mixture. Both complexes were isolated in good yields as air-stable orange solids (Scheme 2). A related complex, which

Scheme 2. Preparation of Complexes 3a−c

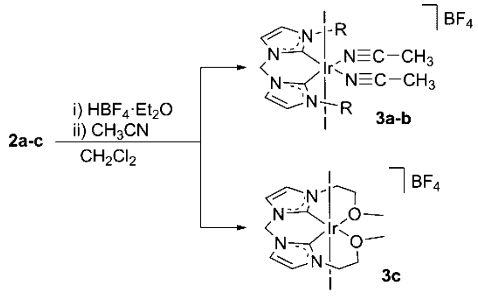

R = -$CH_2CH_2CH_2CH_3$ (**a**), -CH_2CH_2OPh (**b**)

features two coordinated R groups [Ir(I)$_2$\{κ^4*C*,*C*′,*O*,*O*′-(bis-NHC^{OMe})\}] (**3c**; R = $-CH_2CH_2OCH_3$; bis-NHC^{OMe} = methylenebis(*N*,*N*′-bis(2-methoxyethyl)imidazol-2-ylidene)), has been previously reported by us.[9,10]

The formation of the acetonitrile adducts was confirmed by loss of the bidentate acetato ligand, evidenced by the disappearance of the resonances belonging to the CH_3COO^- protons and carbons in ^{1}H NMR and $^{13}C\{^1H\}$ NMR, respectively. Moreover, new peaks corresponding to the acetonitrile ligands emerge in the ^{1}H NMR spectra in deuterated acetone at δ 2.97 and 2.87 ppm for **3a,b**, respectively. The two carbon peaks assigned to the acetonitrile ligands in the $^{13}C\{^1H\}$ NMR spectra are observed at 3.4 ($-CH_3$) and 122.6 (−CN) ppm for **3a** and 3.6 ($-CH_3$) and 123.2 (−CN) ppm for **3b**. ^{19}F NMR further confirms the formation of cationic species **3a,b** by the presence of resonances at δ −150.9 and −150.6 ppm, respectively, due to the BF_4^- counterions.

Suitable crystals of **3a** were grown by slow diffusion of diethyl ether into a saturated acetone solution. The molecular structures obtained by single-crystal X-ray diffraction analysis (Figure 1) confirms the coordination of the acetonitrile ligands in the vacant positions left by the acetate ligand, trans to the NHCs. The iridium center adopts a slightly distorted octahedral geometry. At the apical sites, the iodido ligands form an I1−Ir1−I2 angle of 175.65(4)°. The equatorial plane is completed by both acetonitrile units (N51−Ir1−N41, 84.1(4)°) and the chelating bis-NHC ligand (C12−Ir1−C22, 87.4(6)°). Both imidazole rings exhibit an (open-book) dihedral angle of 137.7(7)°, allowing the IrC_3N_2 metallacycle to achieve a boat conformation.

^{1}H NMR spectra of **3a** in deuterated acetone showed that no apparent exchange between the CH_3CN ligands and the deuterated acetone occurs, as no free acetonitrile was observed, and only one singlet that integrates for six protons was

DOI: 10.1021/om5011726
Organometallics XXXX, XXX, XXX−XXX

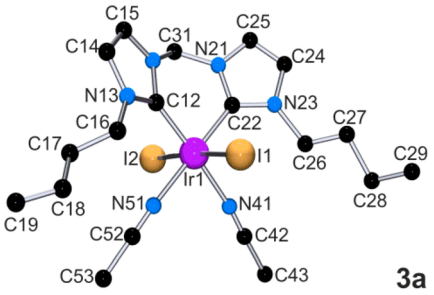

Figure 1. View of cation **3a**. Selected distances (Å) and bond angles (deg): Ir1−I1, 2.6805(11); Ir1−I2, 2.6856(11); Ir1−C12, 1.989(15); Ir1−C22, 2.011(13); Ir1−N41, 2.077(13); Ir1−N51, 2.074(10); C12−Ir1−C22, 87.4(6); N41−Ir1−N51, 84.1(4); C12−Ir1−I1, 90.7(4); C22−Ir1−I1, 91.4(4); I1−Ir1−I2, 175.65(4).

attributed to the methyl protons belonging to the two coordinated acetonitrile ligands. However, it is worth mentioning that the peak corresponding to the coordinated acetonitrile ligands disappears in CD_3CN due to ligand exchange with the solvent.

In addition, two doublets at δ 7.58 and 7.55 ppm (J_{H-H} = 2.2 Hz) and a singlet at δ 6.61 ppm were assigned to the NCH═ protons and the methylene bridge, respectively. The butyl groups on the nitrogen atoms show as the most representative peaks those belonging to the NCH_2 and CH_3 protons, which appear as a multiplet and a triplet (J_{H-H} = 7.4 Hz) centered at δ 4.47 and 1.01 ppm, respectively. $^{13}C\{^1H\}$ NMR spectra in deuterated acetone show a singlet at δ 127.5 ppm corresponding to the carbene carbon and two resonances at δ 122.9 and 122.8 ppm due to the NCH═ carbon atoms. The carbon atoms of the methylene bridge appear at δ 64.4 ppm. The acetonitrile ligands give two resonances at δ 122.6 and 3.4 ppm corresponding to the *C*N and CH_3 carbon atoms.

Attempts to crystallize **3b** (κ^2C,C') by slow diffusion of diethyl ether into a saturated acetone solution resulted in loss of one acetonitrile ligand, thus affording suitable crystals of **3b′** (κ^3C,C',O). This proves the ability of the ethyl phenyl ether functions to coordinate to the metal center and even displace an acetonitrile ligand.

The molecular structure obtained by single-crystal X-ray diffraction analysis (Figure 2) shows the coordination of one acetonitrile ligand in one of the vacant positions trans to the

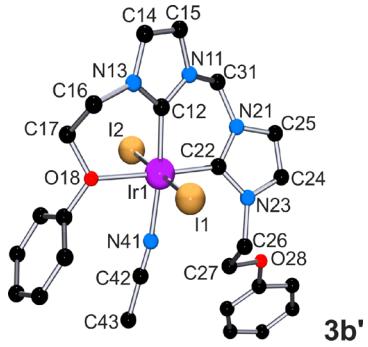

Figure 2. View of cation **3b′**. Select distances (Å) and bond angles (deg): Ir1−I1, 2.674(2); Ir1−I2, 2.672(2); Ir1−C12, Ir1−C22, 1.981(5); 1.974(5); Ir1−O18, 2.239(4); Ir1−N41, 2.082(5); C12−Ir1−C22, 88.6(2); C12−Ir1−O18, 88.98(19); I1−Ir1−I2, 178.577(13).

NHC ligands left by the acetate ligand, while the other is occupied by one of the ether functions of the wingtip groups.

The axial positions are occupied by the two iodido ligands (Ir1−I2, 2.674(2) Å; Ir1−I3, 2.672(2) Å; I1−Ir1−I2, 178.577(13)°), while the bis-NHC ligand is located at the equatorial plane with the NHC rings positioned cis (Ir1−C12, 1.974(5) Å; Ir1−C22, 1.981(5) Å). One of the wingtip groups of the bis-NHC ligand is coordinated to one of the other two available equatorial positions, resulting in an Ir−O bond distance (Ir1−O18, 2.239(4) Å) slightly longer than those recently reported by us for $[Ir(I)_2\{\kappa^4O,C,C',O'$-(bis-$NHC^{OMe})\}]BF_4$[9] (Ir−O, 2.200(3) and 2.204(3) Å). The last available equatorial position, cis to the coordinated oxygen atom, is occupied by an acetonitrile ligand (Ir1−N41, 2.082(5) Å), which leaves one dangling 2-phenoxyethyl substituent. The dihedral angle formed by both imidazole units of **3b** (157.7(2)°) is considerably wider in comparison with that of **3a** (137.7(7)°). The boat conformation of the IrC_3N_2 metallacycle is maintained.

Analogously to complex **3a**, the six-membered metallacycle formed by the bis-NHC ligand and the Ir center adopts a boat conformation. However, in this case, the angle between the two planes that contain each N-heterocyclic ring (160°) is closer to planarity than that in **3a**, probably due to coordination of one of the wingtip groups by its oxygen in **3b**.

^1H NMR spectra of **3b** in deuterated acetone at room temperature suggest a fluxional behavior in solution, which was confirmed by variable-temperature ^1H NMR spectra of **3b** in deuterated acetone (Figure 3). This behavior could be

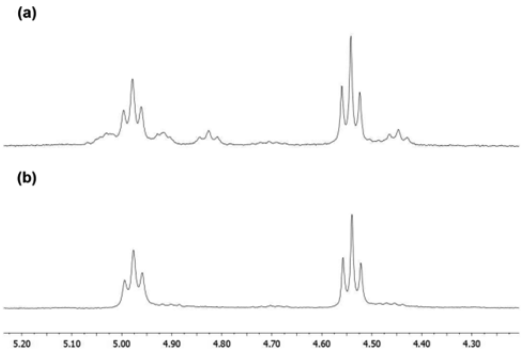

Figure 3. ^1H NMR spectra of the NCH_2 and OCH_2 region for complex **3b** at room temperature with 30 equiv of CH_3CN (a) and without added CH_3CN (b).

attributed to the coordination and dissociation of the ether functions to give a mixture of species **3b** (κ^2C,C'), **3b′** (κ^3C,C',O), and **3b″** (κ^4C,C',O',O) (Supporting Information).

An additional proof that supports the above proposed equilibrium is that the addition of excess CH_3CN (30 equiv) to a solution of **3b** in deuterated acetone affords only one species in the ^1H NMR. The ^1H NMR spectra of **3b** in deuterated acetone with 30 equiv of CH_3CN show two doublets (J_{H-H} = 2.0 Hz) at δ 7.65 and 7.58 ppm corresponding to the NCH═ protons of the N-heterocyclic rings. The hydrogen atoms of the methylene bridge appear at δ 6.65 ppm as a singlet, and the two hydrogen atoms of the NCH_2 and OCH_2 groups at the wingtips appear as multiplets centered at δ 4.95 and 4.52 ppm, respectively.

The isolation of the previously suggested tetracoordinated species **3b″** (κ^4C,C',O,O') was attempted by avoiding the

DOI: 10.1021/om5011726
Organometallics XXXX, XXX, XXX−XXX

addition of CH_3CN; however, the low solubility of the resulting complex in noncoordinating solvents precluded its characterization. ^1H NMR spectra of this complex in acetone show a fluxional behavior that does not resolve at low or high temperatures, which may correspond to a mixture of three species, namely, [Ir(CH_3COCH_3)$_2$(I)$_2$\{κ^2*C*,*C*′-bis(NHC^{OPh})\}], [Ir(CH_3COCH_3)(I)$_2$\{κ^3*C*,*C*′,*O*-bis(NHC^{OPh})\}], and [Ir-(I)$_2$\{κ^4*C*,*C*′*O*′,*O*-bis(NHC^{OPh})\}] (Supporting Information).

The fluxional behavior of **3b** sharply contrasts with the strength of the Ir−O bonds displayed by its analogous complex **3c**. The latter does not show acetonitrile coordination even in the presence of excess acetonitrile at temperatures as high as 80 °C.

$^{13}C\{^1H\}$ NMR spectra of **3b** in deuterated acetone show a peak at δ 123.2 ppm for the carbene carbon and two peaks at δ 123.8 and 123.0 ppm corresponding to the NCH═ carbon atoms. The carbon atom of the NCH_2N bridge appears at δ 64.5 ppm. The two carbon atoms of the acetonitrile ligands appear at δ 123.2 and 3.60 ppm (CH_3 and *C*N, respectively).

Catalytic Studies on the Generation of Hydrogen from Hydrosilanes. Catalysts **3a**,**b** together with **3c** were tested as catalyst precursors for the hydrolysis and methanolysis of a range of organosilanes with the aim of using these reactions as a test bench that would allow assessment of the activity of the three complexes in the generation of hydrogen from silanes (Scheme 3). The three potential catalysts contain bis-NHC

Scheme 3. Hydrolysis or Methanolysis of Silanes

$$R_3SiH + R'OH \xrightarrow{\text{Catalyst}} R_3SiOR' + H_2 \qquad R' = CH_3 \text{ or } H$$

ligands that present wingtip groups with different coordination abilities. Complex **3a** does not contain a coordinating group, while the phenoxy moieties at **3b** behave as hemilabile ligands. On the other hand, the methoxy groups at **3c** are strongly coordinated to the iridium center.

The rate of hydrogen production, generated by hydrolysis or methanolysis of the silane during the catalytic tests, was monitored by measuring the variation of pressure inside the system throughout the reaction by means of a closed reactor flask equipped with a pressure transducer. After hydrogen evolution had ceased, the pressure was released and the resulting solution analyzed by ^1H, $^{13}C\{^1H\}$, and ^{29}Si NMR spectroscopy in order to identify the silicon-containing reaction products.

Initial tests for the hydrolysis of hydrosilanes were carried out using CH_2Cl_2 as solvent; however, the low solubility of the complexes in chlorinated solvents led to low reaction rates ($TOF_{1/2}$ = 111 h^{-1} (**3a**), 86 h^{-1} (**3b**), and 35 h^{-1} (**3c**)). Therefore, acetone was selected as the reaction medium for the hydrolysis tests due to its capacity to dissolve the complexes **3a**−**c**. For comparison purposes, catalysts **3a**−**c** were tested under analogous reaction conditions. $PhMe_2SiH$ (1 equiv) was added to a solution of the corresponding catalysts (1 mol %) and 5 equiv of water in acetone at 298 K. This study revealed that catalyst **3b**, which presents two hemilabile functionalities in the wingtip groups, shows a better activity than that of catalyst **3a**, which contains two noncoordinating N substituents. However, the two strongly coordinating wingtip groups at **3c** seem to thwart its catalytic activity (Figure 4).

Regarding hydrogen generation, alcoholysis has the advantage that no additional solvent is required, as the alcohol acts as

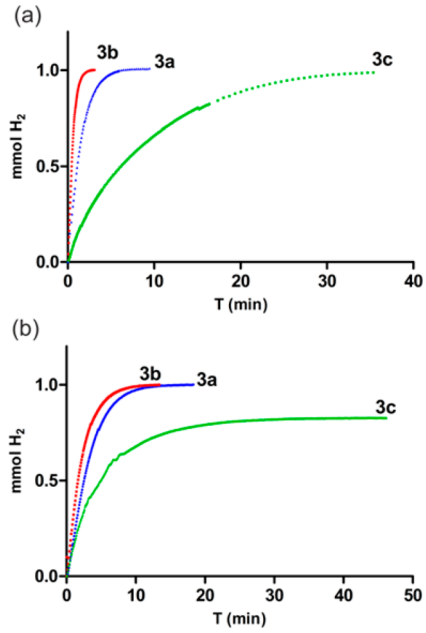

Figure 4. Hydrogen generation (mmol) versus time (min) for the catalytic (a) hydrolysis and (b) methanolysis of $PhMe_2SiH$ using **3a**−**c** (1 mol %) as catalysts and (a) 5.0 equiv of water in 2 mL of acetone or (b) 2 mL of methanol.

solvent and reagent; moreover, the Si−H bond can be easily regenerated from the silyl ether thus obtained.[3d,11]

In order to explore the activity of **3a**−**c** toward silane methanolysis, $PhMe_2SiH$ was added to a solution of the corresponding catalyst in methanol. Remarkably, the reactivity trend described above is maintained for the methanolysis of $PhMe_2SiH$. However, in this case, the difference in activity between **3a** and **3b** is less pronounced (Figure 4b). It is worth mentioning that the production of hydrogen noticeably decreases when methanol is employed instead of water for Si−H splitting, e.g., the best $TOF_{1/2}$ value obtained for the hydrolysis reaction is 7143 h^{-1} for **3b** with $PhMe_2SiH$, while for methanolysis the best $TOF_{1/2}$, also obtained for the same catalyst/silane pair, is 1785 h^{-1} (Tables 1 and 2, entry 2).

Table 1. Hydrolysis of Silanes Catalyzed by 3a−c[a]

entry	silane	catalyst	time (min)	yield of H_2 (%)	$TOF_{1/2}$ (h^{-1})
1	$PhMe_2SiH$	**3a**	6.4	100	2778
2	$PhMe_2SiH$	**3b**	3.0	100	7143
3	$PhMe_2SiH$	**3c**	39.0	99	485
4	Et_3SiH	**3a**	55.4	100	421
5	Et_3SiH	**3b**	88.3	100	202
6	Et_3SiH	**3c**	185.0	72	85.9
7	$(MeO)_3SiH$	**3a**	94.0	64	402
8	$(MeO)_3SiH$	**3b**	94.0	70	422

[a]Reaction conditions: silane (1.0 mmol), water (5 equiv), acetone (2 mL), catalyst (1 mol %) at room temperature.

When a more encumbered silane (Et_3SiH) is employed, two different effects can be observed: (i) significantly lower reaction rates and (ii) higher catalytic activity of **3a** in comparison to **3b**, i.e. better yields with noncoordinating wingtip groups (Figure 5).

DOI: 10.1021/om5011726
Organometallics XXXX, XXX, XXX−XXX

Table 2. Methanolysis of Silanes Catalyzed by 3a–c[a]

entry	silane	catalyst	time (min)	yield of H_2 (%)	$TOF_{1/2}$ (h^{-1})
1	$PhMe_2SiH$	**3a**	18.3	100	1190
2	$PhMe_2SiH$	**3b**	13.4	100	1785
3	$PhMe_2SiH$	**3c**	46.2	83	610
4	Et_3SiH	**3a**	74.0	100	265
5	Et_3SiH	**3b**	173.3	100	98
6	Et_3SiH	**3c**	268.9	95	163
7	$(MeO)_3SiH$	**3a**	106.2	89	167
8	$(MeO)_3SiH$	**3b**	406.0	94	55

[a]Reaction conditions: silane (1.0 mmol), methanol (2 mL), catalyst (1 mol %) at room temperature.

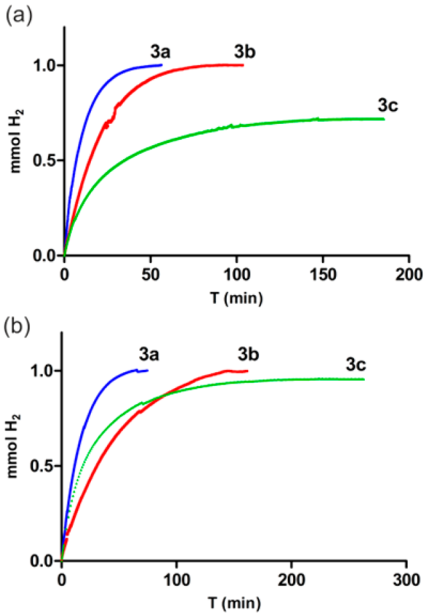

Figure 5. Hydrogen generation (mmol) versus time (min) for the catalytic (a) hydrolysis and (b) methanolysis of Et_3SiH using **3a–c** (1 mol %) as catalyst and (a) 5.0 equiv of water in 2 mL of acetone or (b) 2 mL of methanol.

We observe again that the reactions of silane methanolysis afford smaller values of $TOF_{1/2}$ than their hydrolysis analogues (Tables 1 and 2; entries 4–6). It is remarkable that, in the case of the methanolysis of Et_3SiH, **3c** performs significantly better than **3b** at short reaction times (Figure 5b). This observation suggests that the steric hindrance generated by the wingtip groups may play an important role in the activity of the catalyst when more encumbered hydrosilanes are employed.

Alkoxysilanes were also tested under analogous reaction condition to give low activities and yields even for the most active catalysts (**3a**,**b**) (Tables 1 and 2; entries 7 and 8). The solutions obtained after the hydrolysis of silanes were analyzed by ^1H and ^{29}Si NMR. Remarkably, only the formation of silanols (R_3SiOH) was observed with no traces of $(R_3Si)_2O$.[12] The activities and $TOF_{1/2}$ values here reported compare well with those described in the literature for iridium complexes employing the same hydrosilanes.[2d,3a]

In order to explore the effect of the coordination ability of the wingtip groups on the stability of the catalysts, a reusability study with the most active catalysts, **3a**,**b**, and $PhMe_2SiH$ was undertaken. The catalytic system was reused five times without a significant activity loss of any of the catalysts for the methanolysis reactions. Conversely, for the hydrolysis reaction we observed that the activity of catalyst **3a** gradually decays, becoming especially evident in the fifth cycle. In the next two cycles **3a** completely deactivates, the sixth cycle does not reach a 30% yield, and the seventh cycle shows no conversion whatsoever. This is in contrast with the good activities showed by catalyst **3b** throughout the whole process (Figure 6). A

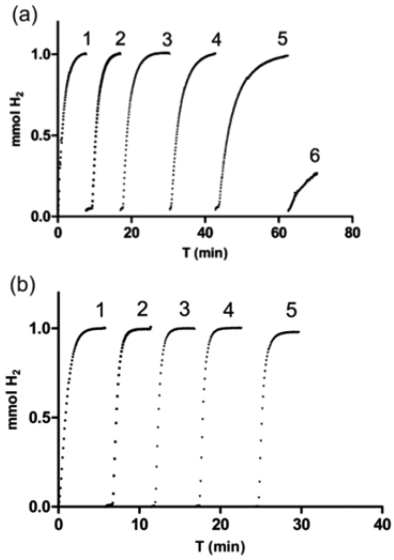

Figure 6. Catalyst recycling experiments of (a) **3a** vs (b) **3b**: hydrogen generation (mmol) versus time (min) for the catalytic hydrolysis of $PhMe_2SiH$ using **3a** (1 mol %) as catalyst and 5.0 equiv of water in acetone. The cycles are numbered from 1 to 6.

plausible explanation for the higher stability showed by catalyst **3b** in comparison with **3a** may be that the stabilization of the active species by the hemilabile wingtip groups results in a longer catalyst lifetime. Notably, this study represents the first example of a reusable homogeneous catalyst for the hydrolysis and methanolysis of silanes.

A catalytic cycle has been proposed on the basis of experimental observations and literature precedents (Figure 7). The fact that the steric hindrance of the silane affects so drastically the reaction rate together with the low activities observed for **3c**, which features strongly coordinating wingtip groups, suggests that coordination of the silane is required. The end-on coordination of hydrosilanes to iridium(III) centers has been described in the literature.[10,13,14] Therefore, we propose the reversible end-on coordination of the hydrosilane through the hydrogen atom as the first step of the catalytic cycle (A–B equilibrium). The next step would be the heterolytic splitting of the Si–H bond, probably assisted by a water molecule following an S_N2-type mechanism,[3a] to give metal hydride species C and cation $R'_3SiOH_2^+$. Subsequently, protonation of the metal hydride by $R'_3SiOH_2^+$ would lead to elimination of molecular hydrogen, with concomitant generation of the corresponding silanol. A plausible mechanism for this last step would be that a proton transfer from $R'_3SiOH_2^+$ to the metal hydride afforded a dihydrogen complex, which would eventually eliminate molecular hydrogen.

An iridium(V)-mediated catalytic cycle has been discarded because, as previously reported by us, oxidative addition of the Si–H bond to **3c**, as a model for A, is not feasible due to the hindered coordination of the silyl moiety.[10]

DOI: 10.1021/om5011726
Organometallics XXXX, XXX, XXX–XXX

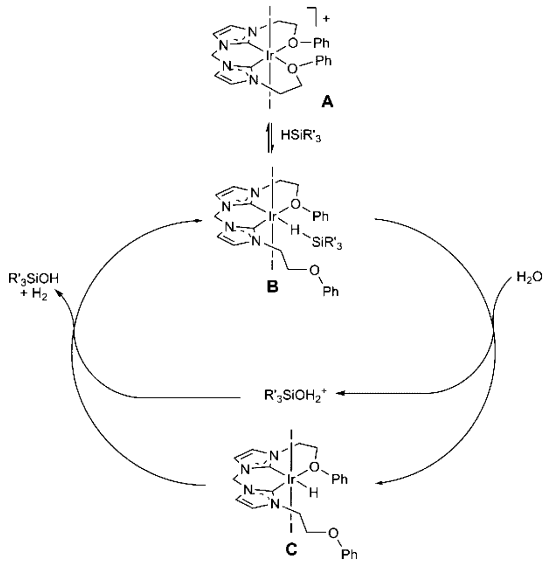

Figure 7. Proposed catalytic cycle with catalyst **3b**.

The higher stability of catalyst **3b** in comparison to that of **3a**, suggested by the reusability tests (Figure 6), indicates a stabilization of the proposed species A, B, or C by ether coordination. Moreover, the better activities showed by **3b** in comparison to **3a** for the least hindered silane ($PhMe_2SiH$) is in agreement with the dynamic behavior observed for **3b** in acetone. The fact that **3a** does not show acetonitrile−acetone exchange points to a better accessibility of the metal center in the case of **3b** (see the Supporting Information). On the other hand, for more sterically hindered silanes, e.g. Et_3SiH, **3a** is slightly more active probably due to the presence of less encumbered wingtip groups in comparison to the case for **3a**.

CONCLUSIONS

The new iridium(III) complexes of general formula $[Ir(CH_3CN)_2(I)_2\{\kappa^2C,C'$-(bis-NHC)$\}]$ have proved to be active catalysts for the hydrolysis and methanolysis of a variety of silanes under mild reaction conditions. The activity of the catalyst is significantly influenced by the coordinating ability of the wingtip groups and the nature of the hydrosilane. Less encumbered silanes seem to promote greater reaction rates, while strongly coordinating groups, as a general rule, hamper the activity of the catalyst. Remarkably, the use of weakly coordinating (hemilabile) wingtip groups leads to a manifest improvement of the catalytic activity when less encumbered silanes were employed but patently hampers the reaction for more sterically hindered silanes.

Catalysts **3a,b** can be reused without a significant loss of activity in the methanolysis of $PhMe_2SiH$. However, in the case of the hydrolysis reaction a progressive drop of the reaction rate throughout the recycling steps and an eventual deactivation of the catalyst were observed for **3a**. This effect was not observed for catalyst **3b**, which seems to retain its activity after five cycles.

In conclusion, the subtle effects of hemilable functions at the N substituents of bis-N-heterocyclic carbene ligands, stabilizing or blocking vacant coordination sites, seem to play a key role in the activity of these catalysts toward hydrogen production from hydrosilanes.

EXPERIMENTAL SECTION

General Considerations. All reactions and manipulations were carried out under an argon atmosphere by using Schlenk-type techniques. Organic solvents were dried by standard procedures and distilled under argon prior to use or obtained oxygen- and water-free from a Solvent Purification System (Innovative Technologies). 1-(2-Phenoxyethyl)-1*H*-imidazole[15] was prepared according to a literature procedure. ^1H NMR and ^{13}C NMR spectra were obtained on a Bruker ARX-300 instrument (300 and 75 MHz, respectively). The chemical shifts are given as dimensionless δ values and are frequency referenced relative to residual solvent peaks for ^1H and ^{13}C and to an external reference of $CFCl_3$ for ^{19}F. Coupling constants J are given in hertz as positive values regardless of their real individual signs. The multiplicity of the signals is indicated as "s", "d", or "m" for singlet, doublet, or multiplet, respectively. $^1H-^1H$-COSY, ^{13}C-APT, $^1H-^{13}C$ HSQC, and $^1H-^{13}C$ HMBC sequences were used for help in the assignments of the ^1H and ^{13}C spectra. Mass spectra and high-resolution mass spectra were obtained on a Esquire 3000+ instrument with ion trap detector interfaced on an Agilent 1100 HPLC analyzer, in electrospray (ES) mode unless otherwise reported. Elemental analyses C/H/N were carried out with a PerkinElmer 2400 CHNS/O analyzer.

Synthesis of 1b. 1-(2-Phenoxyethyl)-1*H*-imidazole (1.05 mmol, 0.331 g) and CH_2I_2 (0.53 mmol, 42 μL) were dissolved in CH_3CN (20 mL). The resulting solution was stirred under reflux for 48 h, after which time the solvent was evaporated under reduced pressure to a volume of 5 mL and precipitated with Et_2O. The remaining residue was washed with Et_2O (3 × 20 mL) and dried in vacuo to give 0.224 g of a white solid (0.25 mmol, 48% yield). ^1H NMR (CD_3CN, 300 MHz): δ 9.69 (s, 2H, $NCHN_{im}$), 7.94 (m, 2H, NCH_{im}), 7.58 (m, 2H, NCH_{im}), 7.31 (m, 4H, 4 × CH_m), 7.00 (m, 6H, 2 × CH_p, 4 × CH_o), 6.81 (s, 2H, CH_2 bridge), 4.60 (m, 4H, NCH_2), 4.32 (m, 4H, OCH_2). ^{13}C NMR (CD_3CN, 300 MHz): δ 158.8 (C_{ipsoAr}), 138.8 (NCHN), 130.6 ($CH_{m\text{-}Ar}$), 124.9 (NCH_{im}), 123.2 (NCH_{im}), 122.5 ($CH_{p\text{-}Ar}$), 115.6 ($CH_{o\text{-}Ar}$), 66.3 (NCH_2), 58.5 (CH_2 bridge), 50.8 (OCH_2). Anal. Calcd for $C_{23}H_{26}I_2N_4O_2$ (644.01): C, 42.86; H, 4.07; N, 8.70. Found: C, 42.76; H, 4.05; N, 8.84.

Synthesis of 2b. $[Ir(\mu\text{-Cl})(COD)]_2$ (0.19 mmol, 0.13 mg) was dissolved in 20 mL of acetonitrile, and subsequently 2 equiv of **1b** (0.38 mmol, 0.34 g), 13 equiv of NaI (2.47 mmol, 0.37 g), and 13 equiv of KOAc (2.47 mmol, 0.24 g) were added. The resulting suspension was refluxed for 3 days. The volatiles were evaporated under reduced pressure, the residue was extracted with CH_2Cl_2 (2 × 25 mL), and the insoluble inorganic salts were filtered off. The solution thus obtained was evaporated in vacuo to afford a residue that was washed with Et_2O (3 × 20 mL). The title compound was isolated as an orange solid in 82% yield (0.139 g, 0.16 mmol). ^1H NMR (CD_2Cl_2, 300 MHz): δ 7.34 (d, 2H, J_{H-H} = 2.1 Hz, $CH_{im\ ext}$), 7.29 (2H, $CH_{Ar\text{-}para}$), 7.26 (4H, $CH_{Ar\text{-}ortho}$), 6.98 (d, J_{H-H} = 2.1 Hz, $CH_{im\ int}$), 6.95 (m, 4H, $CH_{Ar\text{-}meta}$), 6.11 (s, 2H, NCH_2N), 4.83 (m, 4H, NCH_2), 4.40 (m, 4H, OCH_2), 2.01 (s, 3H, CH_3COO). $^{13}C\{^1H\}$ NMR (CD_2Cl_2, 75.5 MHz): δ 190.4 (COO), 158.9 (C_{ipso}), 130.0, 121.7, and 115.2 (CH_{Ar}), 127.9 ($NC_{im}N$), 124.6 ($CH_{im\ ext}$), 119.7 ($CH_{im\ int}$), 68.8 (OCH_2), 63.0 (NCH_2N), 50.3 (NCH_2), 26.2 (CH_3COO). Anal. Calcd for $C_{23}H_{26}I_2N_4O_2$ (644,01): C, 42.86; H, 4.07; N, 8.70. Found: C, 42.76; H, 4.05; N, 8.84.

Synthesis of Complex 2c. Experimental details for the preparation of compound **2c**, as well as its full characterization, can be found in the literature.[9,10]

Synthesis of Complex 3a. The title compound was prepared in 82% yield following a procedure analogous to **3b**. ^1H NMR (acetone-d_6, 300 MHz): δ 7.44, 7.41 (d, 2H, J_{H-H} = 2.2 Hz, $CH_{im\ ext}$), 6.61 (s, 2H, NCH_2N), 4.47 (m, 4H, NCH_2), 2.97 (s, 6H, CH_3CN), 1.99−1.85 (m, 4H, NCH_2CH_2), 1.51 (m, 4H, $NCH_2CH_2CH_2$), 1.01 (t, 6H, J_{H-H} = 7.4 Hz, CH_3). $^{13}C\{^1H\}$ NMR (acetone-d_6, 75.5 MHz): δ 127.5 ($NC_{Im}N$), 122.9 and 122.8 (CH_{im}), 122.6 (CH_3CN), 64.4 (NCH_2N), 52.2 (NCH_2), 33.9 (NCH_2CH_2), 20.6 ($NCH_2CH_2CH_2$), 14.1 (CH_3 terminal), 3.4 (CH_3CN). ^{19}F NMR (acetone-d_6, 282 MHz): δ −150.9 ppm. HRMS (ESI): m/z calcd for $C_{17}H_{27}I_2IrN_5$ ($M^+ - CH_3CN$)

DOI: 10.1021/om5011726
Organometallics XXXX, XXX, XXX−XXX

747.9980, found 748.0035. Anal. Calcd for $C_{19}H_{30}BF_4I_2IrN_6$ (875.32): C, 26.07; H, 3.45; N, 9.60. Found: C, 26.37; H, 3.44; N, 9.34.

Synthesis of Complex 3b. Compound **2b** (0.15 mmol, 0.14 g) was dissolved in 20 mL of CH_2Cl_2, and then $HBF_4{\cdot}Et_2O$ (0.16 mmol, 22 μL) was added dropwise at 0 °C. After the addition the reaction mixture was stirred for 1 h at 0 °C. Subsequently, 10 mL of CH_3CN was added and the reaction mixture was stirred at room temperature for 1 h. Vacuum evaporation of the volatiles afforded a residue, which was washed with Et_2O (3 × 20 mL) and dried under vacuum to give the title compound as an orange solid in 87% yield (0.13 mmol, 0.12 g). ^{1}H NMR (acetone-d_6 with 30 equiv of CH_3CN, 300 MHz): δ 7.67 (d, 2H, J_{H-H} = 2.0 Hz, $CH_{im\ ext}$), 7.58 (d, J_{H-H} = 2.0 Hz, $CH_{im\ int}$), 7.31 (m, 4H, $CH_{Ar\text{-}meta}$), 7.06 (d, 4H, J_{H-H} = 8.2 Hz, $CH_{Ar\text{-}ortho}$), 6.97 (t, 2H, J_{H-H} = 7.4 Hz, $CH_{Ar\text{-}para}$), 6.65 (s, 2H, NCH_2N), 4.95 (m, 4H, NCH_2), 4.52 (m, 4H, OCH_2), 2.87 (s, 6H, CH_3CN). $^{13}C\{^1H\}$ NMR (acetone-d_6, 75.5 MHz): δ 159.2 (C_{ipso}), 130.5 ($CH_{Ar\text{-}meta}$), 127.8 ($NC_{im}N$), 123.8 ($CH_{im\ ext}$),123.2 (CH_3CN), 123.0 ($CH_{im\ int}$), 122.2 ($CH_{Ar\text{-}para}$), 115.4 ($CH_{Ar\text{-}ortho}$), 68.3 (OCH_2), 64.5 (NCH_2N), 51.7 (NCH_2), 3.6 (CH_3CN). ^{19}F NMR (acetone-d_6, 282 MHz): δ −150.6 ppm. HRMS (ESI): m/z calcd for $C_{25}H_{27}I_2IrN_5O_2$ ($M^+ - CH_3CN$) 875.9874, found 875.9914. Anal. Calcd for $C_{27}H_{30}BF_4I_2IrN_6O_2$ (1003.41): C, 32.32; H, 3.01; N, 8.38. Found: C, 31.51; H, 2.78; N, 7.87.[16]

Synthesis of Complex 3c. Experimental details for the preparation of compound **3c**, as well as its full characterization, can be found in the literature.[9,10]

General Procedure for the Hydrolysis of Silanes. The reactions were performed on a Man on the Moon series X102 kit (www.manonthemoon.com) microreactor with a total volume of 14.2 mL placed in an isothermal bath at 298 K.

In a typical procedure, the reactor was charged with a solution of the catalyst (0.01 mmol; 8.8 mg of **3a**, 9.1 mg of **3b** or 8.0 mg of **3c**) and 5 equiv of distilled water (5 mmol, 90 μL) in 2 mL of acetone. The reactor was closed and the pressure measurement started. Once the reading of hydrogen pressure stabilized, the corresponding silane (1.0 mmol; 160 μL of $PhMe_2SiH$, 161 μL of Et_3SiH or 134 μL of $(MeO)_3SiH$) was added with a syringe in one batch. The amount of H_2 generated during the reaction was calculated by means of the ideal gas law: $PV = nRT$. At the end of the reaction the reaction mixture was analyzed by ^{1}H NMR.

General Procedure for the Methanolysis of Silanes. The reactions were performed analogously to the procedure described above for the hydrolysis of silanes, except that in this case the corresponding silane was added to a solution of the catalyst (**3a**, **3b**, or **3c**) in 2 mL of methanol.

General Procedure for Recycling Experiments. The reactions were performed analogously to the procedure described above. After every cycle the system was depressurized and a new 1 equiv of $PhMe_2SiH$ was added. In the case of the hydrolysis experiments 1 equiv of water was previously added to maintain the excess of 5 equiv.

Crystal data for 3a: $[C_{20}H_{31}BCl_2F_4I_2IrN_6]$, monoclinic, $P2_1/c$, a = 12.2648(8) Å, b = 9.2929(6) Å, c = 26.5659(17) Å, β = 95.5340(10)°, Z = 4, M_r = 959.22 g mol^{-1}, V = 3013.8(3) Å^3, D_{calcd} = 2.114 g cm^{-3}, λ(Mo Kα) = 0.71073 Å, T = 100 K, μ = 6.702 mm^{-1}, 25231 reflections collected, 7109 reflections observed (R_{int} = 0.0595), R1(F_o) = 0.0778 ($I > 2\sigma(I)$), wR2(F_o^2) = 0.1772 (all data), GOF = 1.080. CCDC 1034731.

Crystal data for 3b′: $[C_{25}H_{27}BF_4I_2IrN_5O_2]$, monoclinic, $P2_1/n$, a = 15.841(12) Å, b = 12.668(9) Å, c = 16.196(12) Å, β = 116.078(8)°, Z = 4, M_r = 962.33 g mol^{-1}, V = 2919(4) Å^3, D_{calcd} = 2.190 g cm^{-3}, λ(Mo Kα) = 0.71073 Å, T = 100 K, μ = 6.747 mm^{-1}, 32539 reflections collected, 6775 unique reflections (R_{int} = 0.0437), 5644 observed, R1(F_o) = 0.0352 ($I > 2\sigma(I)$), wR2(F_o^2) = 0.1055 (all data), GOF = 0.998. CCDC 1034732.

■ ASSOCIATED CONTENT

Ⓢ Supporting Information

Tables, figures, and CIF files giving X-ray crystallographic details and additional NMR data. This material is available free of charge via the Internet at http://pubs.acs.org.

■ AUTHOR INFORMATION

Corresponding Authors

*E-mail for M.I.: miglesia@unizar.es.
*E-mail for F.J.F.-A.: paco@unizar.es.
*E-mail for L.A.O.: oro@unizar.es.

Notes

The authors declare no competing financial interest.

■ ACKNOWLEDGMENTS

This work was supported by the Spanish Ministry of Economy and Competitiveness (MINECO/FEDER) (CONSOLIDER INGENIO CSD2009-0050, CTQ2011-27593 projects, and "Juan de la Cierva" (M.I.) and Ramón y Cajal (P.J.S.M.) programs) and the DGA/FSE-E07. The authors express their appreciation for support from the Ministry of Higher Education of Saudi Arabia in establishment of the Center of Research Excellence in Petroleum Refining & Petrochemicals at King Fahd University of Petroleum & Minerals (KFUPM) and support from the KFUPM-University of Zaragoza research agreement.

■ DEDICATION

Dedicated to the memory of Prof. Michael F. Lappert, an outstanding and creative scientist, for his many and diverse contributions to organometallic chemistry.

■ REFERENCES

(1) (a) Pouget, E.; Tonnar, J.; Lucas, P.; Lacroix-Desmazes, P.; Ganachaud, F.; Boutevin, B. *Chem. Rev.* **2010**, *110*, 1233−1277. (b) Ojima, I.; Li, Z.; Zhu, J. In *The Chemistry of Organic Silicon Compounds*; Rappoport, S., Apeloig, Y., Eds., Wiley: New York, 1998; Chapter 29. (c) Lickiss, P. D. *Adv. Inorg. Chem.* **1995**, *42*, 147−262. (d) Chandrasekhar, V.; Boomishankar, R.; Magendran, S. *Chem. Rev.* **2004**, *104*, 5847−5910. (e) Murugavel, R.; Walawalkar, M. G.; Dan, M.; Roesky, M. W.; Rao, C. N. R. *Acc. Chem. Res.* **2004**, *37*, 763−774. (f) Murugavel, R.; Voigt, A.; Walawalkar, M. G.; Roesky, H. W. *Chem. Rev.* **1996**, *96*, 2205−2236. (g) Denmark, S. E.; Regens, C. S. *Acc. Chem. Res.* **2008**, *41*, 1486−1499. (h) *Synthesis and Properties of Silicones and Silicone-Modified Materials* (Eds.: Clarson, S. J., Fitzgerald, J. J., Owen, M. J., Smith, S. D., van Dyke, M. E., Eds.; Oxford University Press: Washington, DC, 2003; ACS Symposium Series *838*. (i) Missaghi, M. N.; Galloway, J. M.; Kung, H. H. *Organometallics* **2010**, *29*, 3769−3779. (j) Li, G.; Wang, L.; Ni, H.; Pittman, C. U., Jr. *J. Inorg. Organomet. Polym.* **2001**, *11*, 123−154.

(2) For examples see: (a) Esteruelas, M. A.; Oliván, M.; Vélez, A. *Inorg. Chem.* **2013**, *52*, 12108−12119. (b) Krüger, A.; Albrecht, M. *Chem. Eur. J.* **2012**, *18*, 652−658. (b) Kikukawa, Y.; Kuroda, Y.; Yamaguchi, K.; Mizuno, N. *Angew. Chem., Int. Ed.* **2012**, *51*, 2434−2437. (c) Corbin, R. A.; Ison, E. A.; Abu-Omar, M. M. *Dalton Trans.* **2009**, 2850−2855. (d) Field, L. D.; Messerle, B. A.; Rehr, M.; Soler, L. P.; Hambley, T. W. *Organometallics* **2003**, *22*, 2387−2395. (e) Field, L. D.; Messerle, B. A.; Rehr, M.; Soler, L. P.; Hambley, T. W. *Organometallics* **2003**, *22*, 2387−2395.

(3) (a) Garcés, K.; Fernández-Alvarez, F. J.; Polo, V.; Lalrempuia, R.; Pérez-Torrente, J. J.; Oro, L. A. *ChemCatChem.* **2014**, *6*, 1691−1697. (b) Yu, M.; Jing, H.; Fu, X. *Inorg. Chem.* **2013**, *52*, 10741−10743. (c) Tan, S. T.; Kee, J. W.; Fan, W. Y. *Organometallics* **2011**, *30*, 4008−4013. (d) Han, W.-S.; Kim, T.-J.; Kim, S.-K.; Kim, Y.; Kim, Y.; Nam, S.-W. K; Kang, S. O. *Int. J. Hydrogen Energy* **2011**, *36*, 12305−12312.

DOI: 10.1021/om5011726
Organometallics XXXX, XXX, XXX−XXX

(e) Brunel, J. M. *Int. J. Hydrogen Energy* **2010**, *35*, 3401−3405. (f) Ison, E. A.; Corbin, R. A.; Abu-Omar, M. M. *J. Am. Chem. Soc.* **2005**, *127*, 11938−11939.

(4) (a) Eberle, U.; Felderhoff, M.; Schüth, F. *Angew. Chem., Int. Ed.* **2009**, *48*, 6608−6630. *Angew. Chem.* **2009**, *121*, 6732−6757. (b) Graetz, J. *Chem. Soc. Rev.* **2009**, *38*, 73−82. (c) Service, R. F. *Science* **2004**, *305*, 958−961. (d) Schlapbach, L.; Zuttel, A. *Nature* **2001**, *414*, 353−358.

(5) For examples see: (a) Zahmakiran, M.; Durap, F.; Ozkar, S. *Int. J. Hydrogen Energy* **2010**, *35*, 187−197. (b) Yan, J. M.; Zhang, X. B.; Han, S.; Shioyama, H.; Xu, Q. *Inorg. Chem.* **2009**, *48*, 7389−7393. (c) Chandra, M.; Xu, Q. *J. Power Sources* **2006**, *156*, 190−194. (d) Balema, V. P.; Dennis, K. W.; Pecharsky, V. K. *Chem. Commun.* **2000**, 1665−1666. (e) Kelly, H. C.; Marriott, V. B. *Inorg. Chem.* **1979**, *18*, 2875−2878. (f) Brown, H. C.; Brown, C. A. *J. Am. Chem. Soc.* **1962**, *84*, 1493−1494.

(6) (a) Dröge, T.; Glorius, F. *Angew. Chem., Int. Ed.* **2010**, *49*, 6940−6952. (b) Jacobsen, H.; Correa, A.; Poater, A.; Costabile, C.; Cavallo, L. *Coord. Chem. Rev.* **2009**, *253*, 687−703. (c) Radius, U.; Bickelhaupt, F. M. *Coord. Chem. Rev.* **2009**, *253*, 678−686. (d) Díez-González, S.; Marion, N.; Nolan, S. P. *Chem. Rev.* **2009**, *109*, 3612−3676. (e) Hahn, F. E.; Jahnke, M. C. *Angew. Chem., Int. Ed.* **2008**, *47*, 3122−3172. (f) Frenking, G.; Solà, M.; Vyboishchikov, S. F. *J. Organomet. Chem.* **2005**, *690*, 6178−6204.

(7) (a) Díez-González, S.; Nolan, S. P. *Coord. Chem. Rev.* **2007**, *251*, 874−883. (b) Cavallo, L.; Correa, A.; Costabile, C.; Jacobsen, H. *J. Organomet. Chem.* **2005**, *690*, 5407−5413. (c) Strassner, T. *Top. Organomet. Chem.* **2004**, *13*, 1−20.

(8) Albrecht, M.; Miecznikowski, J. R.; Samuel, A.; Faller, J. W.; Crabtree, R. H. *Organometallics* **2002**, *21*, 3596−3604.

(9) Iglesias, M.; Pérez-Nicolás, M.; Sanz Miguel, P. J.; Polo, V.; Fernández-Alvarez, F. J.; Pérez-Torrente, J. J.; Oro, L. A. *Chem. Commun.* **2012**, *48*, 9480−9482.

(10) Iglesias, M.; Sanz Miguel, P. J.; Polo, V.; Fernández-Alvarez, F. J.; Pérez-Torrente, J. J.; Oro, L. A. *Chem.—Eur. J.* **2013**, *19*, 17559−17566.

(11) For examples of silyl ether reduction see: (a) Volchkov, I.; Lee, D. *J. Am. Chem. Soc.* **2013**, *135*, 5324−5327. (b) Klare, H. F. T.; Oestreich, M.; Ito, J.; Nishiyama, H.; Ohki, Y.; Tatsumi, K. *J. Am. Chem. Soc.* **2011**, *133*, 3312−3315. (c) Kirpichenko, S. V.; Albanov, A. I. *J. Organomet. Chem.* **2010**, *695*, 663−666. (d) Tour, J. M.; John, J. A.; Stephens, E. B. *J. Organomet. Chem.* **1992**, *429*, 301−310. (e) Tamao, K.; Yamauchi, T.; Ito, Y. *Chem. Lett.* **1987**, 171−174. (f) Gevorgyan, V. N.; Ignatovich, L. M.; Lukevics, E. *J. Organomet. Chem.* **1985**, *284*, C31−C32.

(12) For NMR data for R_3SiOH species see: (a) John, J.; Gravel, E.; Hagège, A.; Li, H.; Gacoin, T.; Doris, E. *Angew. Chem., Int. Ed.* **2011**, *50*, 7533−7536. *Angew. Chem.* **2011**, *123*, 7675 −7678. (b) Chauhan, B. P. S.; Sarkar, A.; Chauhan, M.; Roka, A. *Appl. Organomet. Chem.* **2009**, *23*, 385−390. (c) Tokuyasu, T.; Kunikawa, S.; Masuyama, A.; Nojima, M. *Org. Lett.* **2002**, *4*, 3595−3598.

(13) Yang, J.; White, P. S.; Schauer, C. K.; Brookhart, M. *Angew. Chem., Int. Ed.* **2008**, *47*, 4141−4143.

(14) Lalrempuia, R.; Iglesias, M.; Polo, V.; Sanz Miguel, P. J.; Fernández-Alvarez, F. J.; Pérez-Torrente, J. J.; Oro, L. A. *Angew. Chem., Int. Ed.* **2012**, *51*, 12824−12827. *Angew. Chem.* **2012**, *124*, 12996−12999.

(15) Vlahakis, J. Z.; Lazar, C.; Roman, G.; Vukomanovic, D.; Nakatsu, K.; Szarek, W. A. *ChemMedChem.* **2012**, *7*, 897−902.

(16) Although these results are outside the range viewed as establishing analytical purity, probably due to loss of acetonitrile by ether coordination, they are provided to illustrate the best values obtained to date.

DOI: 10.1021/om5011726
Organometallics XXXX, XXX, XXX−XXX